REPORT

Growth responses of mixotrophic giant clams on nearshore turbid coral reefs

Kimberley Mills[1] · Eleanor H. John[1] · Duncan D. Muir[1] ·
Nadiezhda Santodomingo[2] · Kenneth G. Johnson[2] ·
Muhammad Ali Syed Hussein[3] · Sindia Sosdian[1]

Abstract Increasing evidence suggests that nearshore turbid coral reefs may mitigate bleaching of reef building calcifiers and play a critical role in the future of marine biodiversity in coastal areas. However, biomineralization processes on turbid reefs are relatively understudied compared to clear water counterparts and most published work focuses on corals. Here, we investigate how the mixotrophic giant clam *Tridacna squamosa*, a bivalve with ecological, cultural and economic significance, grows across a mosaic of less turbid to turbid reefs in the Coral Triangle. We construct growth chronologies from live and dead collected shells by measuring daily growth increments with petrography and scanning electron microscopy (SEM) to gain insight into growth rate on daily, seasonal and annual scales. We find annual growth is not significantly different across a turbidity gradient when scaled to ontogeny, while seasonal growth highly varies. $K_d(490)$ (a measurement positively correlated with turbidity) and chlorophyll-*a* are likely important factors driving seasonal growth on a turbid reef near a river, compared to sea surface temperature (SST), cloud cover and rainfall on a less turbid reef. On a daily scale, we investigate increment microstructure and spectral characteristics of chronologies, finding a relationship between tidal range and daily increments. Overall, our results indicate that light-enhanced calcification is likely most important in the less turbid reef, compared to heterotrophic feeding in the turbid reef. The trophic plasticity of *T. squamosa* may allow for its sustained growth in marginal conditions, supporting evidence that these habitats serve as important conservation hotspots for diverse reef building taxa.

Keywords Coral triangle · Nearshore turbid reefs · Mesophotic · Sclerochronology · Tridacna · Biomineralization

✉ Kimberley Mills
millsk3@cardiff.ac.uk

1 School of Earth and Environmental Sciences, Cardiff University, Cardiff, UK

2 Natural History Museum, London, UK

3 Borneo Marine Research Institute, Universiti Malaysia Sabah, Kota Kinabalu, Malaysia

Introduction

Coral reefs provide critical ecosystem services to millions of people worldwide but are under threat due to multiple anthropogenic stressors acting at a local to global level (Hughes et al. 2017). Recently, turbid nearshore reefs have shown resilience in the face of increasing thermal stress and have been proposed as important ecological refugia (Cacciapaglia and van Woesik 2016; Zweifler et al. 2021). Although traditionally perceived as 'sub-optimal' (Kleypas et al. 1999), these reefs sustain high live coral cover and typically show resilience to bleaching during elevated temperatures as suspended particles protect corals from damaging high irradiance (Perry and Larcombe 2003; Waheed and Hoeksema 2013; Browne et al. 2019; Sully and van Woesik 2020). Moreover, recent evidence from the fossil record shows early diversification of ancient coral communities occurred in turbid reefs, with the persistence of high diversity lasting over geologic timescales (Santodomingo et al. 2016). Yet, responses to turbid reefs are confounding among coral taxa (Bainbridge et al. 2018). Although turbidity can cause slower growth (Risk and Sammarco 1991)

or loss of photosynthetic endosymbionts (Dallmeyer et al. 1982), some mixotrophic species adapt by utilising resources to offset stress from particle loads (Anthony 2000; Fox et al. 2018). However, aside from corals, little is known about how other key reef builders calcify in turbid reefs. A robust understanding of different organisms and functional groups is required because individual responses result in ecosystem-wide effects (Bainbridge et al. 2018).

Giant clams (Cardiidae: Tridacninae) are large and long-lived symbiont bearing bivalves, distributed throughout the Indo-Pacific (Rosewater 1965). They fulfil critical roles in tropical reef communities due to their contributions to the structure, complexity and ecology of reefs (Neo et al. 2015). Their rapid (daily increment widths of 5–200 μm) and continuous shell growth (Ma et al. 2020) has long been attributed to the photosynthetic rate of their endosymbiotic zooxanthellae (Klumpp and Griffiths 1994). Therefore, changes in growth are expected to be sensitive to external environmental conditions that directly or indirectly alter light exposure (Sano et al. 2012). In some species, translocated photosynthates from endosymbionts satisfy all daily metabolic energy requirements (Jantzen et al. 2008). However, tridacnids are mixotrophs and like many bivalves, take up particulate organic matter (POM) (Klumpp et al. 1992) through filter-feeding. The balance of autotrophy and heterotrophy to total energy requirements changes depending on inter- and intraspecific differences in size, photosynthetic potential (Jantzen et al. 2008), and ontogeny (Klumpp and Griffiths 1994). Compared to most tridacnids, *Tridacna squamosa* (fluted giant clam) is a 'true mixotrophic species' due to its reduced photosynthetic activity, showing a reliance on a heterotrophic strategy to satisfy its metabolic needs within its range (Tedengren et al. 2000; Jantzen et al. 2008). Indeed, the survival of *T. squamosa* may be comparable or even higher under turbidity relative to clearer water (Guest et al. 2008; Yong et al. 2022). However, how growth and biomineralization processes of *T. squamosa* vary between turbid and clear waters and external mechanisms controlling these processes are not understood. Increasing understanding of how giant clams respond to local stressors is required for conservation strategies under continued environmental change (Watson and Neo 2021).

Petrographic microscopy, scanning electron microscopy (SEM) and laser scanning confocal microscopy (LSCM) methods have revealed daily growth increments in both the inner- (Watanabe et al. 2004; Aubert et al. 2009; Elliot et al. 2009; Schwartzman et al. 2011; Sano et al. 2012; Ayling et al. 2015; Hori et al. 2015; Warter et al. 2015; Arias-Ruiz et al. 2017; Gannon et al. 2017; Warter and Müller 2017; Ma et al. 2020; Yan et al. 2020; Yan et al. 2021; Zhao et al. 2021; Liu et al. 2022) and outer layers of giant clam shells (Duprey et al. 2015; Komogoe et al. 2018; Killam et al. 2021). Shell growth chronologies constructed from

these daily increments are important alongside powerful geochemical techniques (e.g. LA-ICP-MS) in reconstructing highly time-resolved profiles of water temperature (e.g. Arias-Ruiz et al. 2017), productivity (e.g. Elliot et al. 2009), paleoweather (Komagoe et al. 2018; Yan et al. 2020) and diurnal light cycles (Sano et al. 2012), among others. The refinement of identification of growth increments is important in different environments and ensures accuracy of time-series analysis (Warter and Müller 2017). Yet, the environmental controls on variation in daily growth increments are little understood and the potential of tridacnid shell growth chronologies on their own remains largely untapped (Zhao et al. 2021).

In this work, we investigate the growth rate of *T. squamosa* in turbid and clear reefs on annual, seasonal and daily scales. We focus on measuring daily increment widths and investigate the microstructure of increments in shells collected alive from two contrasting reef sites—a turbid reef near a river outlet and a less turbid reef. We select the Coral Triangle region of northeast Borneo (Sabah, Malaysia) as our study site because turbid reefs occupy about 30% of reefs within the region (Sully and van Woesik 2020). To disentangle potential external environmental drivers of growth between the less turbid and turbid reef, we compare shell growth chronologies and their spectral characteristics with in situ and remote sensing environmental data. We further investigate growth across a gradient of turbidity by exploring growth trends in shells collected dead at four additional reef sites.

Materials and methods

Regional setting

Darvel Bay (4° 5356′ N, 118° 2646′ E) is the largest semi-enclosed bay on the eastern coast of Sabah and is connected to the Pacific Ocean through the Sulu-Celebes Sea (Fig. 1). It is within the northern corner of the Coral Triangle, a region noted for its high levels of marine biodiversity and endemism (DeSilva et al. 1999; Veron 2000). Coral reefs here are dominated by small patch and fringing reefs developed around the coastline and numerous islands (Ditlev et al. 1999). Mangrove ecosystems are associated with small freshwater catchment areas and prevail near Sakar Island and around the estuaries of the Silabukan and Tingkayu rivers, which play important roles in carrying wastewater discharge and land-based pollutants into the coastal area (Saleh et al. 2007). Climatic conditions are controlled by the Indo-Australian monsoon system, divided into the southwest monsoon between May to September (dry season) and northeast monsoon from November to March (wet season) (Saleh et al. 2007). The tidal range is mesotidal (between 2 and 4 m)

Fig. 1 False colour composite map (bands 7/4/2) of sample sites in Darvel Bay (wet season). Enlarged points correspond to key localities Baik and Triangle, where *Tridacna squamosa* were collected alive. River plume originating from the Tingkayu river in bright blue
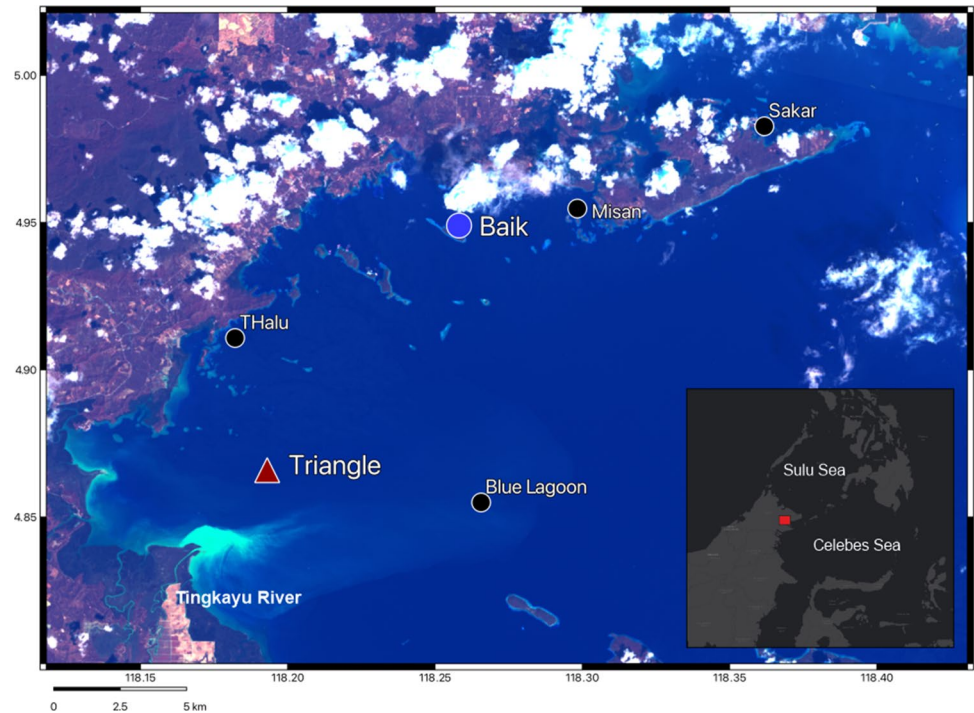
(Santodomingo et al. 2021) and strong tidal currents control water circulation and runoff (Saleh et al. 2007).

Study sites and samples

We carried out an in-depth comparison of daily growth rate for *T. squamosa* at two key reef sites in Darvel Bay—Baik and Triangle (Fig. 1). Baik is proximal to a fish farm, and activities at the site include recreational diving. It has low sediment input and is indicative of a less turbid reef. Triangle is approximately 3.5 km from the mouth of the Tingkayu River, which discharges sediment to the site at low tide. Four shells were extracted alive at Baik and Triangle in April 2019 (SSbaik and SSct, respectively) and February 2020

(NS207 and ZW156, respectively) between depths of 5 and 8.5 m (Tables 1, S1).

In addition, eight shells were collected dead from the seafloor at Baik (SS01BBT), Triangle (SS03BCT, SS03BCT) and four additional locations across a gradient of turbidity (Sakar (SS02ASN), Misan (SS01ASM), THalu (SS01ATH) and Blue Lagoon (SS01ABH)) (Fig. 1; Tables 1, S1). Although these shells appeared to record in situ environmental change and bioerosion assessment of shells collected from specific environments showed similar features, we highlight the caveat that they may have been translocated by local fishermen or wave action post-mortem. Due to these uncertainties, shells collected dead were used only for comparison of overall growth and not employed for further analysis to explore the relationship between growth

Table 1 Coral reef sampling sites in Darvel Bay (East Sabah, Malaysia)

Site	Collection status	Adjacent coastal environment and human activities	Annual mean $K_d(490)$
Baik	L, D	Fish farm/recreational diving	0.09
Triangle	L, D	Near Tingkayu river outlet	0.30
Blue Lagoon	D	Semi-atoll/recreational diving	0.08
THalu	D	Mangroves/conservation area	0.13
Misan	D	Mangroves/estuary	0.10
Sakar	D	Mangroves/urban	0.39
Semporna reefs	U	Recreational diving	0.06

Nearby coastal environment, human activities and mean annual Kd(490) (2019–2020) are shown.

L live collected shells, *D* dead collected shells, *U* unknown collection status

and environmental variables. To broaden the comparison to a wider region, another two shells from Semporna reefs (SEMA, SEMB) situated south of Darvel Bay were obtained from collections at Amgueddfa Cymru—National Museum Wales (NMW). It is unknown if the shells from Semporna were collected dead or alive.

In situ measurements of water clarity at each site were estimated with a turbidity meter (Nephelometric Turbidity Units: NTU) and Secchi disc in the dry season of 2019, yet prolonged drought experienced throughout southeast Sabah during early 2019 (Payus et al. 2020) meant that measurements were atypically low. Therefore, we define turbidity herein based on the amount of suspended particles using the diffuse attenuation coefficient of spectral irradiance at 490 nm wavelength $K_d(490)$ (Table 1). This choice is supported by studies such as Loila et al. (2019), who used remote sensed $K_d(490)$ values as robust indicators of differences in turbidity on coral reefs. We define low turbidity as mean annual $K_d(490) < 0.2 \text{ m}^{-1}$ and the turbidity threshold as mean annual $K_d(490) > 0.2 \text{ m}^{-1}$ (e.g. Yu et al. 2016). We interpret this parameter alongside remote sensed chlorophyll-*a* concentrations, shown to be controlled by river runoff in the wet season (Chen et al. 2007).

All shells were cut into ~ 1–2-cm-thick slices along the axis of maximum growth (transversal from umbo to upper shell margin) (Figs. 2a, b) with either a HC Evans and Son (Eltham) LTD (250 mm blade, 1 mm thickness) or Logitech GTS1 Thin Section Cut-Off diamond saw. Thin sections (60 μm thickness) of the inner layer cut perpendicular to the direction of growth were prepared from slices, ground with 1000 grit sandpaper, and polished with 0.3 μm alumina oxide (Fig. 2c). To improve visibility of features, sections were etched with 0.5% HCL for 15 s. Prior to analysis, dead collected shells were investigated for diagenesis with Raman Spectroscopy and SEM. Evidence of original aragonite was found in all shells and alteration to calcite not detected (Supplemental for more information; Figs. S1, S2). Lengths of shells ranged between 98.59 to 362.62 cm and heights 67.27 to 215.08 cm (umbo to margin).
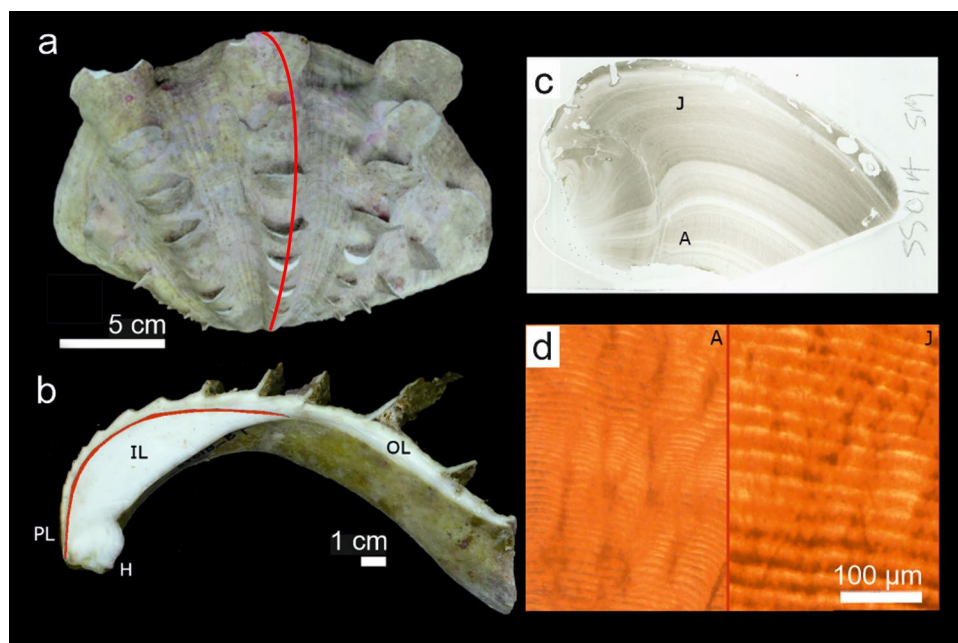
Environmental data

We used in situ and satellite remote sensed data to characterize environmental factors for the last year of growth (LYOG) in shells collected alive from Baik and Triangle (Table S2). Sea surface temperature (SST) and light intensity (lux) were characterized with a HOBO temperature and light logger and data collected every 10–15 min between 2019 and 2020. Tide data were sourced from the Sea Level Monitoring Facility (www.ioc-sealevelmonitoring.org/bgraph.php?code=ms006&output=tab&period=30&endtime=2022-01-31-) at Lahad Datu (stn. ms006). Cloud cover, salinity, chlorophyll-*a*, $K_d(490)$, rainfall and additional SST data for 2018–2019 were sourced from Google Earth Engine (GEE) or the National Oceanic and Atmospheric Administration (NOAA) database (Table S2).

Shell growth chronologies

Shell growth chronologies were assembled from the daily increments of thirteen *T. squamosa* shells to determine daily growth rate. We used a mixed-method approach to image increments with a light microscope (Leica DMR) (10–40 × magnification) and a Zeiss Sigma HD field

Fig. 2 **a** Valve of *Tridacna squamosa* with red vertical line indicating section location. **b** Transversal section from umbo to upper shell margin highlighting the inner layer (IL), outer layer (OL), pallial line (PL) and hinge (H). **c** Thin section of the inner shell layer denoting first growth (juvenile growth, J) and last growth (adult growth, A). **d** Daily growth increments under transmitted light microscopy (20 x magnification) from first (J) and last growth (A)

emission gun SEM (1500× magnification) at the School of Earth and Environmental Sciences, Cardiff University. For SEM, sections were coated with 20 nm gold–palladium alloy using a BIO-RAD SC500 sputter coater and growth increments and their microstructure observed at high vacuum with an acceleration voltage 10 kV and aperture size 30 μm. Images were obtained along the height of the inner layer and montaged on Microsoft Image Composite Editor (ICE) (light microscope) or Oxford Instruments AZtec 6.0 software (SEM).

The number and width of daily increments were determined from light microscopy and SEM images using ImageJ 1.53 (Schneider et al. 2012) and Coorecorder 9.8 (Cybis) (Maxwell and Larsson 2021) software. By using sets of images from both methods and software, multiple counts were obtained for each shell (Table S3). To reduce sampling bias when comparing shells collected alive with environmental data, a second person also counted sets of increments from these shells. Final mean shell growth chronologies were compiled from multiple counts that met certain criteria, which was based on how many increments could be defined (Supplemental for more information; Table S4; Figs. S3, S4).

Data analysis

Data analysis was carried out in RStudio Version 4.0.3 (R Core Team 2020) unless otherwise specified. The R code is available from the Mendeley Data Repository at https://doi.org/10.17632/mbjzc2nbsn.1. We used a dimensionless standardized growth index (SGI) to control for ontogenetic decelerated growth rates (e.g. Jones et al. 1986). Often used in studies of bivalves (e.g. Butler et al. 2013), including giant clams (Zhao et al. 2021), the SGI is an estimation of how growth deviates from the average growth trend (see Schöne 2003). We applied the SGI to our data as ages of samples likely covered life stages from juvenile to adult. We investigated SGI values on daily, seasonal and annual scales. To examine differences in annual growth, a one-way analysis of variance (ANOVA) and post hoc Tukey test were performed between shells pooled into the seven reefs. Assumptions of ANOVA were checked for normality and homogeneity of variance using Shapiro–Wilk's test, QQ (quantile–quantile) plots of standardized residuals and Bartlett's test. On a monthly scale, SGI values were plotted with monthly averaged environmental data for the LYOG in the shells collected alive at Baik and Triangle. These data were explored as added-variable (AV) plots because they control for the variability of other explanatory variables when plotting the effect of x on y. They therefore more accurately show relationships because other variables in the model are adjusted for (Draper et al. 1966). Principal component analysis (PCA) was also performed on environmental data

for time periods corresponding to LYOG to explore annual and seasonal relationships, allowing the number of variables under investigation to be reduced. Finally, we used spectral analysis to investigate daily growth with tidal cycles in frequency space in Baik and Triangle because tidal patterns are thought to be expressed in the daily increments of *T. squamosa* (Evans 1972). Multi-taper method spectral analysis (MTM) (Thompson 1982) was carried out in K-Spectra v.3.9.3 (SpectraWorks) to extract dominant frequencies. Cycles were analysed with significance of spectral peaks at 95–99% compared to red noise background.

Results

Environmental data

Mean SST for 2019–2020 at Baik and Triangle was 29.53 °C and 30.01 °C, respectively (Fig. 3a). Throughout the year, monthly SST varied between 28.11 °C and 30.47 °C at Baik and 28.93 °C and 30.91 °C at Triangle, peaking at the end of the dry season and generally dropping towards the end of the wet season. Light intensity (lux) corresponded with SST in Baik and showed a peak in October, varying between monthly lux of 7122.50 and 16,444.75 throughout the year compared to 7285.83 lux and 13,705.91 lux for Triangle (Fig. 3b). However, it is important to consider that we could not retrieve data for lux between August and October for Triangle, as the HOBO logger was lost. Precipitation showed a bimodal distribution pattern, with maximum rainfall towards the beginning of the dry- and mid-wet season in both sites (Fig. 3f). Chlorophyll-*a* (Fig. 3d) generally corresponded to $K_d(490)$ (Fig. 3c) in both sites, but maximum monthly values were higher at Triangle (4.19 mg m^{-3}, 0.51 m^{-1}, respectively) than Baik (1.06 mg m^{-3}, 0.14 m^{-1}, respectively). Cloud cover was similar between sites (Fig. 3e), peaking in June and dropping during the late wet season in March. Although patterns were similar in 2018–2019, prolonged drought in early 2019 revealed atypically low cloud cover (51%, both sites) and rainfall (62.98 mm Baik; 43.35 mm Triangle) in February 2019. Sea surface salinity (SSS) showed a partial inverse behaviour with rainfall (Fig. S5).

We used PCA to further explore relationships between environmental variables at Baik and Triangle. PCA defined two principal components covering 77.1% of the cumulative variance (Fig. 4). PC1 accounted for 43.9% of variance, with highest negative association of SST and cloud cover and highest positive association of salinity and rainfall, while PC2 accounted for 33.2% of variance and showed highest negative association of chlorophyll-*a* and $K_d(490)$ and positive association of cloud cover and SST. Baik and Triangle generally clustered into two groups regardless of season. However, two points that represented the dry season of 2019,
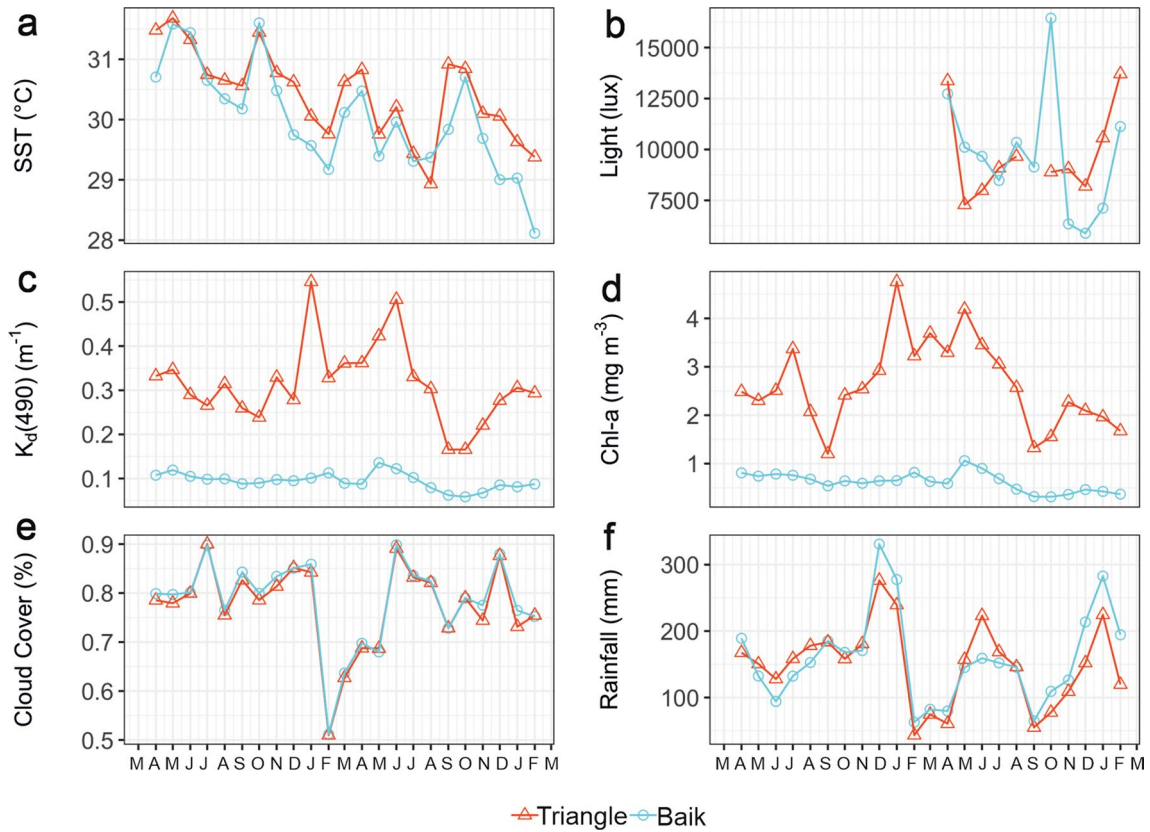
Fig. 3 a Monthly average sea surface temperature (SST), **b** light (lux), **c** K_d(490) (m^{-1}), **d** chlorophyll-*a* (mg m^{-3}), **e** cloud cover (%) and **f** rainfall (mm) from Baik and Triangle reefs in Darvel Bay for 2018–2020. Environmental data shown relate to last year of growth (LYOG) for samples collected live in April 2019 and February 2020

Fig. 4 Principal component analysis (PCA) for environmental data: monthly average sea surface temperature (SST), K_d(490) (m^{-1}), chlorophyll-*a* (mg m^{-3}), cloud cover (%) and rainfall (mm) from Baik and Triangle reefs in Darvel Bay, showing the loading of each variable (black arrows) and PCA scores (points) of each season for 2018–2020. Superimposed 95% confidence ellipsoids contain group points. Point sizes represent quality of representation of each individual point
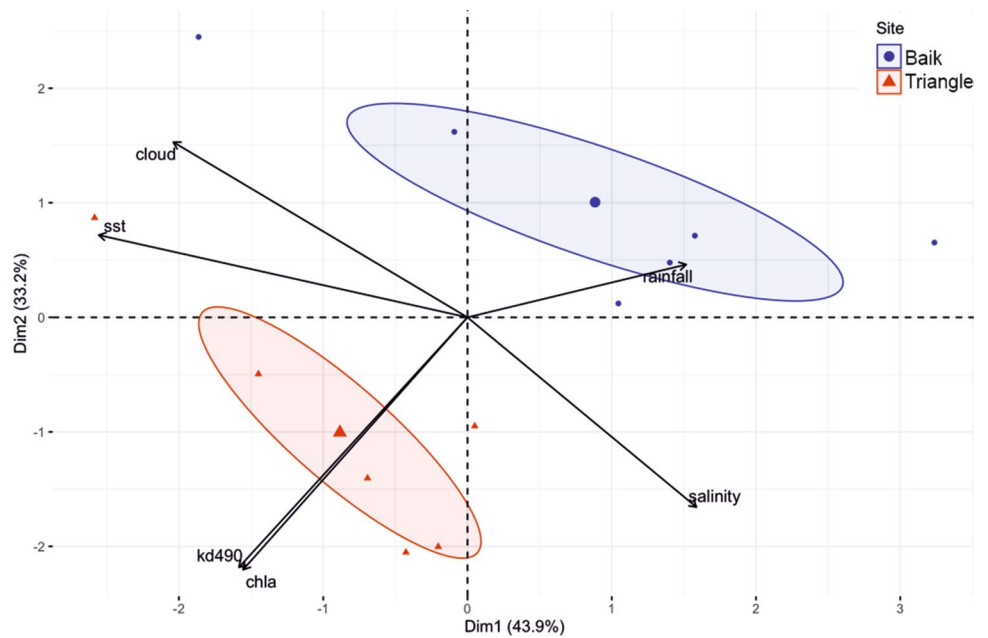
when anomalous drought was experienced, were positioned in the top left quadrant and did not cluster with others.

Growth increment microstructure

The microstructure of daily growth increments in the inner shell layer varied among the thirteen *T. squamosa* shells depending on collection site. Two distinct microstructures of daily increments were noted: Type 1—Paired growth couplets, consisting of a thicker- and thinner layer, delineated by crystalline structure, similar to the thicker prismatic layer and thinner layer with oblique crystals described by Gannon et al. (2017) (Fig. 5a, c); Type 2—Two adjacent organic rich growth lines delineating a band and intersecting an irregular or cone complex crossed lamellar microstructure (Taylor et al. 1969) (Fig. 5b, d). Type 1 was generally found in shells from the Triangle reef, while Type 2 was common in Baik, Blue Lagoon, THalu, Misan, Sakar and Semporna. Despite these differences, overall observations of the outer shell layer showed an identical microstructure in every specimen that consisted of a crossed lamellar arrangement (Taylor et al. 1969).

The microstructure observed in Type 1 showed a stronger delineation than Type 2. Thus, it was easier to observe, measure and count growth increments and in turn, data from shells with Type 1 had lower errors (calculated by value 1 subtracted from value 2, divided by value 1) between individual counts (0.74–2.37%). In contrast, the recorded variability in counting and measuring the least visible increments of Type 2 demonstrates that these increments were harder to distinguish. A comparison of the relationship between d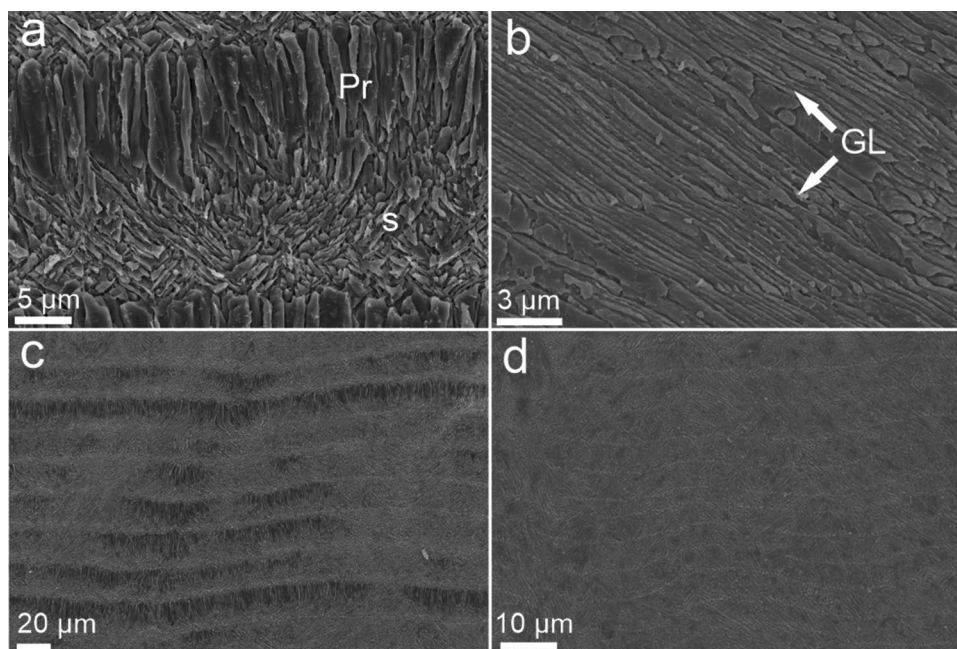ays alive and daily growth (μm) for individual counts that made up final mean growth chronologies of live collected *Tridacna squamosa* shells SSbaik (Baik, 2019 collected), SSct (Triangle, 2019 collected), NS207 (Baik, 2020 collected) and ZW156 (Triangle, 2020 collected) is shown in Fig. 6. For instance, the SSbaik shell showed a very large offset of 880 increments between petrographic and SEM approaches (error 44.88%). However, data were similar between observer counts in the juvenile region of growth (Fig. 6a).

Annual shell growth

Lifespan of all shells was estimated between 0.72 (262 days) and 7.23 (1726 days) years (Table S4). Seven shells were under 3 years, indicating the juvenile life stage, while six were over 3 years, which may indicate adulthood (Lucas 1994). Shell growth chronologies over 3 years generally showed a concave-down shape and could be divided into two broad stages: Stage 1—Rapid acceleration at start of life and Stage 2—Deceleration in or after 3 years (Fig. 7). Younger shells that presumably had not reached latter growth stages showed no concavity but continued rapid growth or no relationship with days alive.

Mean shell growth rates over lifespan varied greatly and ranged from 3.91 ± 1.39 to 8.13 ± 3.37 mm/yr (Table S4), corresponding to daily increment widths between 2.02 and 41.40 μm (mean 14.90 μm/day). In all shells, mean annual growth in the first year of life was 6.28 mm/yr ($n = 11$), 5.51 mm/yr ($n = 7$) in 0–2 yr, 5.18 mm/yr ($n = 2$) in 2–4 yr, 3.58 mm/yr ($n = 1$) in 4–6 yr, following age-related deceleration of growth (Fig. 7). Shells from Semporna ($n = 2$) showed pooled fastest overall mean annual growth (7.46 mm/yr),

Fig. 5 SEM images of the microstructure of paired daily increments in *Tridacna squamosa* from Triangle reef **a**, **c**, consisting of a simple prismatic layer (Pr) and layer with smaller crystals (s). **b**, **d** In Baik shells, there is a complex crossed lamellar microstructural arrangement with faint growth lines (GL) running perpendicular to first order lamellae
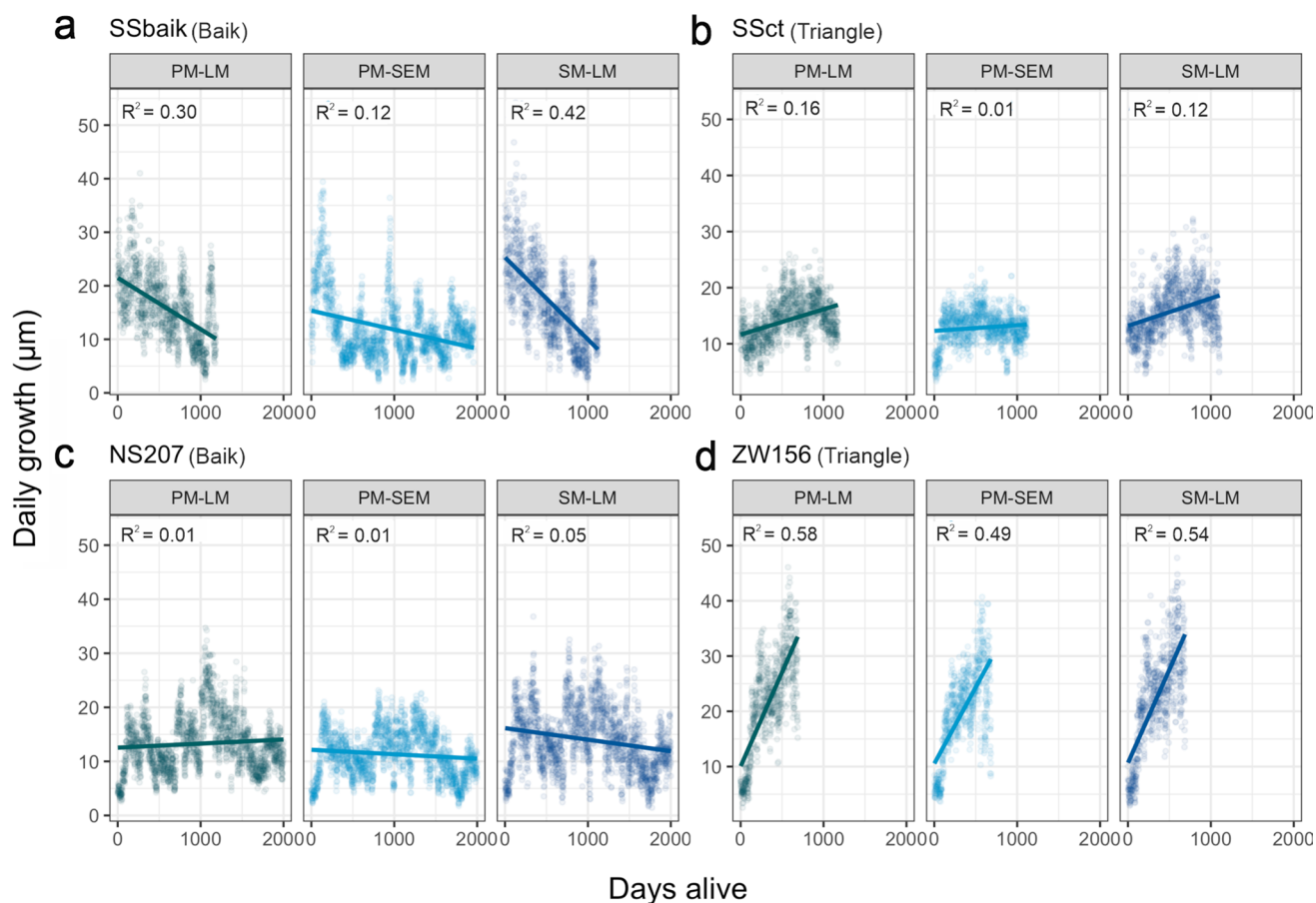
Fig. 6 Comparison of relationship between days alive and daily growth (µm) for individual counts of live collected *Tridacna squamosa* shells SSbaik (Baik, 2019 collected) **a**, SSct (Triangle, 2019 collected) **b**, NS207 (Baik, 2020 collected) **c**, ZW156 (Triangle, 2020 collected) **d** PM-LM = primary counter, measurement tool ImageJ, light microscopy images; PM-SEM = primary counter, measurement tool ImageJ, SEM images; SM-LM = secondary counter, measurement tool ImageJ, light microscopy images

followed by those from Triangle ($n = 4$) (6.16 mm/yr), Misan 5.41 mm/yr ($n = 1$), Baik 4.61 mm/yr ($n = 3$), Sakar 4.26 mm/yr ($n = 1$), and THalu 3.91 mm/yr ($n = 1$). Among individual shells, ZW156 from Triangle showed fastest mean growth (21.55 µm/day), while SS01ATH from THalu (10.72 µm/day) grew slowest (Fig. 7a, b).

SGI values revealed contrasting results to raw growth rates and showed similar minimum and maximum values between all *T. squamosa* shells irrespective of site or age (Fig. 7c, d). One-way ANOVA and post hoc Tukey test confirmed no significant differences in SGI over lifespan between shells from different sites ($p > 0.05$) (Table. S5).

**Seasonal shell growth and environmental relationships**

Distinct temporal patterns that were most prominent at a seasonal level were revealed in live collected shell chronologies where exact dates of death were known. The most striking difference was acceleration of growth that generally occurred in the wet season for Baik, while a seasonal trend in Triangle was less clear (Fig. 8). Undated SGI chronologies from dead collected shells at the same sites revealed similar seasonal acceleration in Baik, while Triangle showed smaller fluctuations and shorter-term cycles throughout the year (Fig. S6).

Undated SGI chronologies from dead shells collected at additional sites generally showed a similar seasonal range of SGI values to live collected shells (Fig. S7). The shell from Blue Lagoon revealed positive SGI values in the second year of growth, compared to only negative SGI values in the third year, while the shell from Misan showed a distinct peak in the third year of growth. Younger shells at THalu and Semporna that were under 3 years showed a short deceleration in the second year of growth before death.

AV plots revealed significant relationships between monthly SGI and cloud cover ($p < 0.05$) and SST ($p < 0.05$) in one Baik shell (SSBaik) (Fig. S8) and salinity ($p < 0.01$) and rainfall ($p < 0.01$) in the additional older Baik shell (NS207) (Fig. S9). In contrast, shells from Triangle (ssCT; ZW156) showed no significant correlation between tested

Fig. 7 All mean shell growth chronologies derived from daily growth increment widths of live (**a**, **c**) and dead (**b**, **d**) collected *Tridacna squamosa* for comparison of shell growth over lifespan. Measurements are presented by rate of daily growth (μm) (**a**, **b**) and detrended growth rates shown in the dimensionless unit of the standardized growth index (SGI) (**c**, **d**). Lines are smoothed (span 0.1) and colours represent sample. Shells younger than 365 days are excluded from SGI values
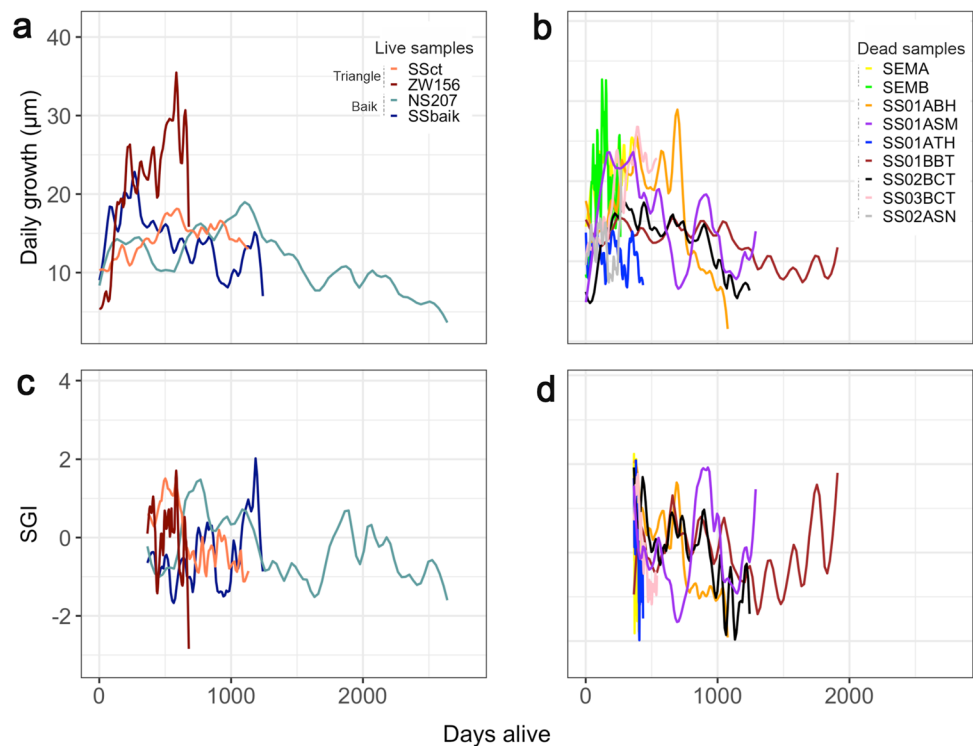
environmental variables and SGI values (Figs. S10, S11). Nonetheless, we did note a degree of synchronization with bimodal chlorophyll-*a* and K_d(490) peaks in ZW156, while growth appeared relatively consistent year-round in ssCT (Fig. S12).

Spectral analysis

Multi-taper method (MTM) spectral analysis was applied to daily SGI values and tidal range to search for similarity of periodicities in frequency space. Daily growth increments in Triangle shells were characterized by high-frequency significant peaks corresponding to periods of ~2–3 days and spectra revealed several similarities with daily maximum sea level (Fig. 9). Significant peaks in Baik shells occurred over a wider range of frequencies corresponding to periods of ~2–6 days and showed less similarity with tidal spectra (Fig. S13).

Discussion

Multi-method approach to sclerochronology in giant clams

In this study, we established shell growth chronologies for thirteen giant clam shells based on counting and measuring widths of daily growth increments with a mixed-method approach (petrography and SEM). To reduce uncertainty,

increments were counted multiple times with different software and live collected shells cross-checked by a secondary person. However, large offsets existed between counts in some samples, which could be attributed to either differences in microstructure that reduced growth increment visibility or visualization of bands between approaches.

Molluscan shell microstructure is underpinned by genetic mechanisms but is further influenced by external environmental factors (Clark et al. 2020). Size and shape of biomineral units may change depending on temperature (Milano et al. 2017; Höche et al. 2020, 2021), light attenuation (Pätzold et al. 1991) and food supply (Clark et al. 2020). Here, we found two distinct microstructures of daily increments for the inner shell layer of *T. squamosa:* Type 1 in the Triangle reef, which consisted of paired daily growth couplets with a thicker- and thinner layer delineated by crystalline structure and Type 2 in other reef sites, with two adjacent growth lines cutting a complex crossed lamellar microstructural arrangement that was either irregular or cone (Taylor et al. 1969) and running perpendicular to first order lamellae (Agbaje et al. 2017). Delineation of daily increments from Type 1 shells was clearer than Type 2, and this was reflected in the differences between individual counts (Table S3). Distinctly demarcated paired increments that vary in morphology along one growth increment like Type 1 have previously been recorded for *T. gigas* (Pätzold et al. 1991; Gannon et al. 2017) and are presumably driven by the daily light cycle (Sano et al. 2012). The thicker prismatic layer is thought to be deposited in the daytime when symbiotic algae allow
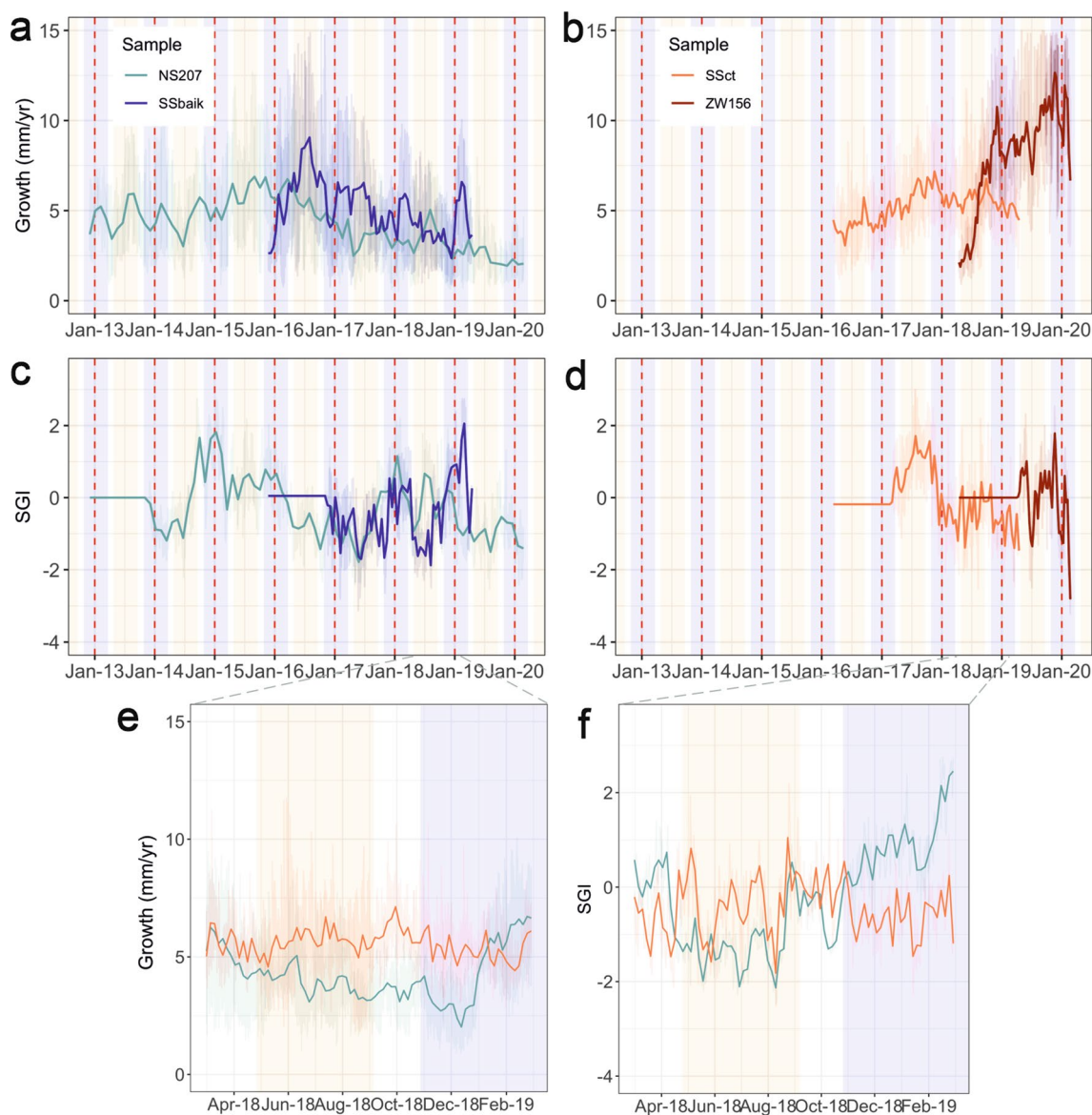
Fig. 8 Dated mean shell growth chronologies derived from daily growth increment widths for *Tridacna squamosa* collected from Baik (blue lines) (**b**, **d**) and Triangle (red lines) (**a**, **c**) reefs in 2019 (SSct, SSbaik) and 2020 (ZW156, NS207). Measurements from raw data are presented in mm/yr (**a**, **b**) and detrended growth rates shown in the dimensionless unit of the standardized growth index (SGI) (**c**, **d**). Red dashed vertical lines represent one year of growth, and pur- ple and orange bars represent wet and dry seasons, respectively. Raw growth (**e**) and SGI chronologies (**f**) showing only last year of growth (LYOG) in Baik (SSbaik) (blue line) and Triangle (SSct) (red line) reveal seasonal variation between the two sites. Raw data are represented by pale lines, and data after smoothing are represented by bold lines

light-enhanced calcification, while the thinner layer may calcify at night when less light is available for photosynthetic processes (Sano et al. 2012). Although Pätzold et al. (1991) described a similar microstructure with faint growth lines like Type 2, they only reported its occurrence near the umbo and not throughout other regions of the shell. We found Type 2 to be common in early stages of growth when growth was faster, presumably a continuation of the simple crossed lamellar microstructural arrangement of the outer shell layer. Although this concurs with reports of less defined crystalline boundaries indicating faster deposition of microstructural components (Gannon et al. 2017), Type 2 continued into adulthood in many shells and Type 1 only recorded in Triangle, which may relate to tidal rhythm (discussed below).

Apart from microstructure, differences in visibility of daily growth increments in giant clam shells have also been attributed to method specific issues. For example, changes
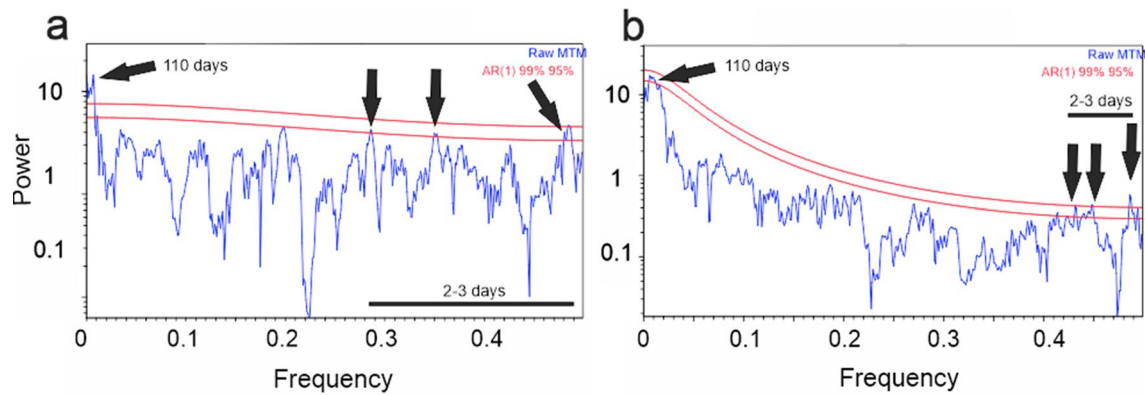
Fig. 9 Multi-taper method (MTM) power spectra of **a** daily maximum tide (m) and **b** daily SGI growth chronology of Triangle reef shell ZW156 in frequency space. AR(1) significance peaks are set to 95 and 99% and represented to a red noise background. Significant peaks labelled with arrows and identified in approximate days in relation to frequency (1/day)

in focal length and low fluorescence of shell material under LSCM (Zhao et al. 2021). We used high-resolution SEM imaging across the entirety of the inner layer of each shell because this method allows singular daily increments to be revealed in detail in secondary electron images (Welsh et al. 2011). Shell regions whose daily increments remained unclear under SEM are likely a true feature of the sample instead of an artefact of sampling technique. We additionally found the boundary between the outer- and inner shell layers (i.e. the pallial line) distinct under SEM (Fig. S14), similar to other studies (Gannon et al. 2017; Ayling et al. 2017). Yet, this was sometimes unclear under light microscopy, which may be attributed to variation in focal length due to the presence of a highly topographic complex crossed lamellar microstructural arrangement. These results emphasize the importance of applying a multi-method approach in counting daily growth increments of giant clams because large unveiled offsets could severely obstruct interpretation for high-resolution studies.

Shell growth mediated by ontogeny

A challenge in the study of sclerochronology is to disentangle vital effects and externally forced growth signatures (e.g. temperature) (Schöne 2003). As for many bivalves, physiological processes of tridacnids change with the onset of sexual maturity and energy priorities switch between growth and reproduction (Jones et al. 1986). Over time, increments become tightly packed and rate and year to year amplitude of growth decreases (Romanek and Grossman 1989; Arias-Ruiz et al. 2017; Zhao et al. 2021). In this study, shell growth chronologies accounting for ontogenetic growth were investigated before applying the SGI. We found most shells over approximately three years old demonstrated rapid acceleration at the beginning of life and reduction in growth in or after three years (Fig. 7). Although delayed onset of sexual

maturity (approximately 10 years) and subsequent deceleration of growth has been recorded for *Tridacna maxima* (Jones et al. 1986; Romanek et al. 1987; Chambers 2007) and *T. gigas* (Klump and Griffiths 1994; Lucas 1994), the switch between juvenile and adult growth phases may occur earlier in other species (Lucas 1994). While our shells are young (~ 1–7 yr) relative to the natural lifespan of *Tridacna* spp. (several decades) (Rosewater 1964), growth curves in some samples may indicate early onset maturity for *T. squamosa*.

Environmental influences on shell growth

Our results revealed mean shell growth rates from seven reefs that ranged from 3.91 ± 1.39 to 11.67 ± 3.97 mm/yr, corresponding to daily increment widths between 2.02 and 41.40 μm (mean of 14.90 μm/day). Despite shells being collected from a range of reefs subject to varying turbidity, results were generally consistent with those in the literature for modern and cultured shells, showing mean daily increment widths of 3–32.7 μm for measurements of the inner layer of *T. squamosa* and other Tridacnidae (Aubert et al. 2009; Elliot et al. 2009; Schwartzmann et al. 2011; Ariaz-Ruiz et al. 2017; Gannon et al. 2017; Yan et al. 2020; Zhao et al. 2021) (Fig. 10). Moreover, removal of ontogenetic growth signals using the SGI revealed no significant differences across annual growth rate from shells at any of our sites over lifespan. However, we do caution the uncertainties of the interpretation of the dead collected shells from the seafloor and it is possible that they were translocated post-mortem.

Influences on annual shell growth

One explanation for similar annual SGI values across sites may be related to the trophic plasticity documented for *T.*

Fig. 10 Mean daily growth rate (µm) of the inner shell layer for Darvel Bay and Semporna Tridacnidae (current study) compared to published growth values. Reef location *SCS* Southern South China Sea, *PNG* Papua New Guinea, *GBR* Great Barrier Reef. Sample zhao_md3 = Zhao et al. (2021); yan_XB10 = Yan et al. (2020); arias-ruiz_GSL14_19 = Ariaz-Ruiz et al. (2017); gannon_K-133 = Gannon et al. (2017); gannon_PT-1 = Gannon et al. (2017); elliot_Tgplam = Elliot et al. (2009); schwartzman = Schwartzmann et al. (2011), aubert = Aubert et al. (2009). Error bars represent standard deviation if available
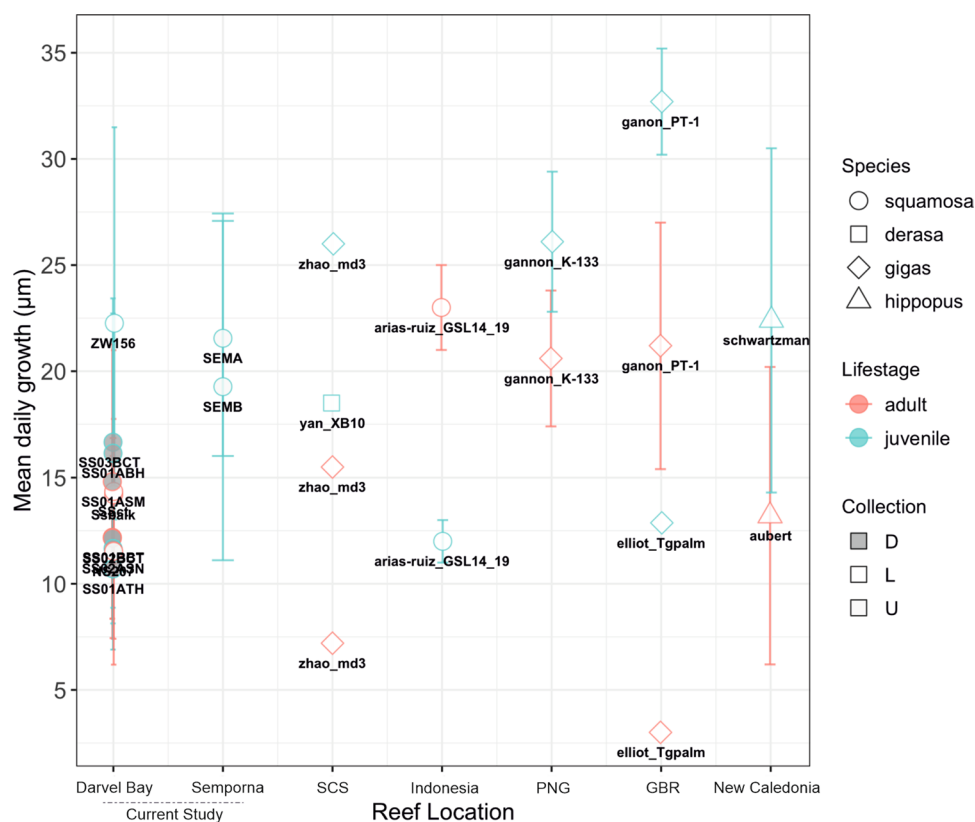
squamosa. Unlike some giant clam species who are functional autotrophs, *T. squamosa* has a photoautotrophic range that is extended by heterotrophy (Jantzen et al. 2008). Although contributions of heterotrophy to total energy requirements in tridacnids change depending on ontogenetic stage and size (Fisher et al. 1985; Klump et al. 1992; Klumpp and Griffiths 1994; Yau and Fan 2012), *T. squamosa* is unusual because it has significantly lower photosynthetic potential irrespective of age and is more reliant on filter-feeding (Jantzen et al. 2008). It is known to increase rates of filter-feeding with depth (Tedengren et al. 2000) and is common on the deeper fore-reef compared to other species, which are abundant in shallow (< 3 m) reef flat (Roa-Quiaoit 2005). Our results lend weight to *T. squamosa* surviving and potentially thriving in turbid reefs and concur with other studies (Guest et al. 2008; Yong et al. 2022), who reported the species can survive well and even accelerate growth on impacted reefs.

Influences on monthly shell growth

On the contrary, at a seasonal level we found substantial site-to-site variability between the shells collected alive from Baik and Triangle, indicating that different environmental factors may play some role in regulation of intra-annual growth trends. At the less turbid reef Baik, growth generally accelerated in the wet season and monthly SGI

values negatively correlated with temperature, cloud cover, rainfall and salinity. Although in previous studies of giant clams increment widths positively correlate with SST (Aubert et al. 2009; Duprey et al. 2015; Komagoe et al. 2018; Zhao et al. 2021), the negative correlation found between SGI and temperature in Baik may relate to depressed growth above a thermal tolerance threshold of 27 °C (Schwartzman et al. 2011; Killam et al. 2021). As monthly SST varied between 28.11 °C and 30.47 °C at Baik, increment thickness could become erratic and a stress reaction initiated (Schwartzman et al. 2011). Another explanation may be the small variation in SST throughout the year (~ 2 °C), considered negligible in terms of contribution to growth rate (Gannon et al. 2017). As such, SST may play an indirect role in modulation of growth of our shells due to its relationship with light. A positive correlation between light and growth has been observed in several tridacnid species on diurnal—(Sano et al. 2012; Yan et al. 2021) to seasonal scales (Lucas et al. 1989). Yan et al. (2021) found co-variance of daily growth rate with outgoing longwave radiation (OLR), but no significant correlation with SST for *Tridacna derasa*, indicating local effective solar radiation, is more important than SST in determination of increment width. Our results of an inverse relationship between monthly SGI and cloud cover indicate at least some light dependence on growth in Baik caused by photosynthetic activity of endosymbionts.

Seasonal rainfall within Darvel Bay is enhanced by southwest (dry season) and northeast (wet season) monsoons. Rainfall may indirectly influence growth by washing particulate matter into the region, increasing local turbidity and impeding photosynthetic processes (Gannon et al. 2017). High-resolution paleoweather reconstructions show abrupt decreases in daily increment thickness due to cold upwelling and strong wave action from typhoon and tropical cyclone activity (Komagoe et al. 2018; Yan et al. 2020). Although monthly SGI in Baik shows a negative relationship with rainfall, periods of reoccurring accelerated growth in the mid to late wet season may be attributed to enhanced vertical mixing after increased rainfall, bringing nutrient rich sub-surface waters to the surface, coupled with subsequent increased solar irradiance (Gannon et al. 2017; Yan et al. 2020). While Baik is indicative of a low turbid reef and K_d(490) and chlorophyll-a do not increase to the same extent as Triangle, we propose that a sequence of events similar to that recorded by Gannon et al. (2017) following: (1) higher rainfall during the early wet season, (2) elevated K_d(490) and chlorophyll-a, (3) increased sunlight, may result in favourable growing conditions.

Unlike Baik, shells from Triangle lacked any statistically significant relationship between monthly SGI and environmental variables. Yet, we did note a positive association between SGI and chlorophyll-a and K_d(490) in some months. Triangle is a naturally turbid reef situated approximately 3.5 km from the mouth of the river

Tingkayu, which discharges sediment to the site at low tide. During ebb tide, freshwater carrying sediment loads are directly discharged seaward to the reef at the surface, while density gradients generating two-layer circulation patterns move saltwater landward at the bottom (Saleh et al. 2007). Sediment input is likely land derived POM produced in the river basin by different mechanisms (e.g. freshwater productivity and remains of plants and microorganisms) and mineral sediment (Bainbridge et al. 2018). In similarity to mixotrophic corals (Fox et al. 2018), elevated chlorophyll-a concentrations at Triangle may indicate $T.\ squamosa$ utilises chlorophyll-a as a key contributor towards metabolic requirements in reduced photic depth. Local irradiance may be of less importance for $T.\ squamosa$ compared to other giant clam species, and it can sustain growth in turbid reefs if a suitable local food source is available.

Influences on daily shell growth

At a daily scale, spectral characteristics of SGI chronologies revealed similarities with tidal range at Triangle. Significant spectral peaks occurred at around two to three days corresponding closely to peaks in maximum daily tide. Tidal rhythms are known to leave characteristic daily growth or geochemical patterns in many bivalves, such as

differentiation of increment widths that relate to spring-neap variability or daily tidal emergence (Goodwin et al. 2001) and trace element cyclicity (Warter and Müller 2017; de Winter et al. 2022). It has recently been suggested that under natural conditions the circadian clock genes of some bivalves may also run at tidal frequency, indicating behavioural patterns relating to a circadian cycle can be modulated by tidal rhythm (Tran et al. 2020). Based on this hypothesis, the presence of paired daily increments in Triangle shells may relate to reef sediment flux controlled by a circadian rhythm paced to tides that result in variable light intensities. The thicker prismatic layer presumably related to higher irradiance may be accreted during flood tide, when clear water is transported offshore to the reef. At ebb tide when suspended sediment is transported to the reef lowering photic depth, smaller crystals could be deposited. However, more work is needed to elucidate the relationship between short-term tidal cycles and daily growth increments in tridacnids.

Conclusion

In this study, we provide the first assessment of growth in giant clams from turbid reefs using a mixed method approach. We investigated daily growth increments in thirteen *Tridacna squamosa* shells from different coral reef sites with varying degrees of turbidity. Similarities were found in annual growth rate between clear and turbid reefs, while there were differences in seasonal growth trends, indicating that an interplay of different environmental factors may regulate intra-annual growth between reefs. At a daily scale, we found differences in microstructure and spectral characteristics of daily increments, which may relate to tidal variability at the turbid site near a river source. Our results do not indicate that turbidity negatively influences growth but are consistent with sustained growth, which may relate to the trophic plasticity of *T. squamosa*. This work supports growing evidence that resilient marginal habitats with elevated turbidity may serve as important conservation hotspots and our results are useful in the context of management and conservation for *T. squamosa* under changing future oceanic conditions. Although encouraging, we cannot ascertain what this may mean for other parameters important for survival, such as skeletal density. More work is needed on different tridacnid species to better understand the multiple environmental and physiological influences of turbidity.

Declarations

References

Agbaje OBA, Wirth R, Morales LFG, Shirai K, Kosnik M, Watanabe T, Jacob DE (2017) Architecture of crossed-lamellar bivalve shells: the southern giant clam (*Tridacna derasa*, Röding, 1798). R Soc open sci 4:170622. https://doi.org/10.1098/rsos.170622

Anthony KRN (2000) Enhanced particle-feeding capacity of corals on turbid reefs (Great Barrier Reef, Australia). Coral Reefs 19:59–67. https://doi.org/10.1007/s003380050227

Arias-Ruiz C, Elliot M, Bézos A, Pedoja K, Husson L, Cahyarini SY, Cariou E, Michel E, La C, Manssouri F (2017) Geochemical fingerprints of climate variation and the extreme La Niña 2010–11 as recorded in a Tridacna squamosa shell from Sulawesi. Indonesia Palaeogeog Palaeoclimatol Palaeoecol 487:216–228. https://doi.org/10.1016/j.palaeo.2017.08.037

Aubert A, Lazareth CE, Cabioch G, Boucher H, Yamada T, Iryu Y, Farman R (2009) The tropical giant clam *Hippopus hippopus* shell, a new archive of environmental conditions as revealed by sclerochronological and δ18O profiles. Coral Reefs 28:989–998. https://doi.org/10.1007/s00338-009-0538-0

Ayling BF, Chappell J, Gagan MK, McCulloch MT (2015) ENSO variability during MIS 11 (424–374 ka) from *Tridacna gigas* at Huon Peninsula, Papua New Guinea. Earth Planet Sci Lett 431:236–246. https://doi.org/10.1016/j.epsl.2015.09.037

Bainbridge Z, Lewis S, Bartley R, Fabricius K, Collier C, Waterhouse J, Garzon-Garcia A, Robson B, Burton J, Wenger A, Brodie J (2018) Fine sediment and particulate organic matter: a review and case study on ridge-to-reef transport, transformations, fates, and impacts on marine ecosystems. Mar Pollut Bull 135:1205–1220. https://doi.org/10.1016/j.marpolbul.2018.08.002

Browne NK, Braoun C, McIlwain J, Nagarajan R, Zinke J (2019) Borneo coral reefs subject to high sediment loads show evidence of resilience to various environmental stressors. PeerJ 7:e7382. https://doi.org/10.7717/peerj.7382

Butler PG, Wanamaker AD, Scourse JD, Richardson CA, Reynolds DJ (2013) Variability of marine climate on the North Icelandic Shelf in a 1357-year proxy archive based on growth increments in the bivalve Arctica islandica. Palaeogeog Palaeoclimatol Palaeoecol 373:141–151. https://doi.org/10.1016/j.palaeo.2012.01.016

Cacciapaglia C, van Woesik R (2016) Climate-change refugia: shading reef corals by turbidity. Glob Change Biol 22:1145–1154. https://doi.org/10.1111/gcb.13166

Chambers CN (2007) Pasua (*Tridacna* maxima) size and abundance in Tongareva Lagoon, Cook Islands. SPC Trochus Information Bulletin 13:7–12

Chen Z, Muller-Karger FE, Hu C (2007) Remote sensing of water clarity in Tampa Bay. Remote Sens Environ 109:249–259

Clark MS, Peck LS, Arivalagan J et al (2020) Deciphering mollusc shell production: the roles of genetic mechanisms through to ecology, aquaculture and biomimetics. Biol Rev 95:1812–1837. https://doi.org/10.1111/brv.12640

Dallmeyer DG, Porter JW, Smith GJ (1982) Effects of particulate peat on the behavior and physiology of the Jamaican reef-building coral *Montastrea annularis*. Mar Biol 68:229–233. https://doi.org/10.1007/BF00409589

de Winter NJ, Killam D, Fröhlich L, de Nooijer L, Boer W, Schöne BR, Thébault J, Reichart GJ (2022) Ultradian rhythms in shell composition of photosymbiotic and non-photosymbiotic mollusks. EGUsphere. https://doi.org/10.5194/egusphere-2022-576

Ditlev H, De Silva MWRN, Ridzwan AR, Toerring D, Widt S (1999) Hard corals of Darvel Bay. In: De Silva MWRN, Rahman RA, Mustafa S, Cabanban AS (eds) A study of living marine resources of Darvel Bay, Sabah, Malaysia. Borneo Marine Research Unit, Universiti Malaysia Sabah, Kota Kinabalu, pp 51–57

Draper NR, Smith H, Pownell E (1966) Applied regression analysis. Wiley, New York

Duprey N, Lazareth CE, Dupouy C, Butscher J, Farman R, Maes C, Cabioch G (2015) Calibration of seawater temperature and δ18Oseawater signals in *Tridacna* maxima's δ18Oshell record based on in situ data. Coral Reefs 34:437–450. https://doi.org/10.1007/s00338-014-1245-z

Elliot M, Welsh K, Chilcott C, McCulloch M, Chappell J, Ayling B (2009) Profiles of trace elements and stable isotopes derived from giant long-lived *Tridacna gigas* bivalves: Potential applications in paleoclimate studies. Palaeogeog Palaeoclimatol Palaeoecol 280:132–142. https://doi.org/10.1016/j.palaeo.2009.06.007

Evans JW (1972) Tidal Growth Increments in the Cockle Clinocardium nuttalli. Science 176:416–417. https://doi.org/10.1126/science.176.4033.416

Fisher CR, Fitt WK, Trench RK (1985) Photosynthesis and respiration in *Tridacna Gigas* as a function of irradiance and size. Biol Bull 169:230–245. https://doi.org/10.2307/1541400

Fox MD, Williams GJ, Johnson MD, Radice VZ, Zgliczynski BJ, Kelly ELA, Rohwer FL, Sandin SA, Smith JE (2018) Gradients in primary production predict trophic strategies of mixotrophic corals across spatial scales. Curr Biol 28:3355-3363.e4. https://doi.org/10.1016/j.cub.2018.08.057

Gannon ME, Pérez-Huerta A, Aharon P, Street SC (2017) A biomineralization study of the Indo-Pacific giant clam *Tridacna gigas*. Coral Reefs 36:503–517. https://doi.org/10.1007/s00338-016-1538-5

Goodwin DH, Flessa KW, Schone BR, Dettman DL (2001) Cross-calibration of daily growth increments, stable isotope variation, and temperature in the gulf of california Bivalve Mollusk Chione cortezi: implications for paleoenvironmental analysis. Palaios 16:387–398. https://doi.org/10.1669/0883-1351(2001)016%3c0387:CCODGI%3e2.0.CO;2

Guest JR, Todd PA, Goh E, Sivalonganathan BS, Reddy KP (2008) Can giant clam (*Tridacna squamosa*) populations be restored on Singapores heavily impacted coral reefs? Aquatic Conserv: Mar. Freshw Ecosyst 18:570–579. https://doi.org/10.1002/aqc.888

Höche N, Peharda M, Walliser EO, Schöne BR (2020) Morphological variations of crossed-lamellar ultrastructures of Glycymeris bimaculata (Bivalvia) serve as a marine temperature proxy. Estuar Coast Shelf Sci 237:106658. https://doi.org/10.1016/j.ecss.2020.106658

Höche N, Walliser EO, de Winter NJ, Witbaard R, Schöne BR (2021) Temperature-induced microstructural changes in shells of laboratory-grown Arctica islandica (Bivalvia). PloS one 16:e0247968. https://doi.org/10.1371/journal.pone.0247968

Hori M, Sano Y, Ishida A, Takahata N, Shirai K, Watanabe T (2015) Middle Holocene daily light cycle reconstructed from the strontium/calcium ratios of a fossil giant clam shell. Sci Rep 5:8734. https://doi.org/10.1038/srep08734

Hughes TP, Barnes ML, Bellwood DR et al (2017) Coral reefs in the Anthropocene. Nature 546:82–90. https://doi.org/10.1038/nature22901

Jantzen C, Wild C, El-Zibdah M, Roa-Quiaoit HA, Haacke C, Richter C (2008) Photosynthetic performance of giant clams, Tridacna maxima and T. squamosa. Red Sea Mar Biol 155:211–221. https://doi.org/10.1007/s00227-008-1019-7

Jones DS, Williams DF, Romanek CS (1986) Life history of symbiont-bearing giant clams from stable isotope profiles. Science 231:46–48. https://doi.org/10.1126/science.231.4733.46

Killam D, Al-Najjar T, Clapham M (2021) Giant clam growth in the Gulf of Aqaba is accelerated compared to fossil populations. Proc R Soc B 288:20210991. https://doi.org/10.1098/rspb.2021.0991

Kleypas JA, Mcmanus JW, Meñez LAB (1999) Environmental Limits to coral reef development: where do we draw the line? Am Zool 39:146–159. https://doi.org/10.1093/icb/39.1.146

Klumpp D, Griffiths C (1994) Contributions of phototrophic and heterotrophic nutrition to the metabolic and growth requirements of four species of giant clam (Tridacnidae). Mar Ecol Prog Ser 115:103–115. https://doi.org/10.3354/meps115103

Klumpp DW, Bayne BL, Hawkins AJS (1992) Nutrition of the giant clam *Tridacna gigas* (L.) I. Contribution of filter feeding and photosynthates to respiration and growth. J Exp Mar Biol Ecol 155:105–122. https://doi.org/10.1016/0022-0981(92)90030-E

Komagoe T, Watanabe T, Shirai K, Yamazaki A, Uematu M (2018) Geochemical and microstructural signals in giant clam *Tridacna maxima* recorded typhoon events at Okinotori Island. Japan J Geophys Res Biogeosci 123:1460–1474. https://doi.org/10.1029/2017JG004082

Liu C, Zhao L, Zhao N, Yang W, Hao J, Qu X, Liu S, Dodson J, Yan H (2022) Novel methods of resolving daily growth patterns in giant clam (*Tridacna* spp.) shells. Ecol Ind 134:108480. https://doi.org/10.1016/j.ecolind.2021.108480

Loiola M, Cruz ICS, Lisboa DS, Mariano-Neto E, Leão ZMAN, Oliveira MDM, Kikuchi RKP (2019) Structure of marginal coral reef assemblages under different turbidity regime. Marine Environmental Research 147: Lough JM, Barnes DJ (1992) Comparisons of skeletal density variations in Porites from the central Great Barrier Reef. J Exp Mar Biol Ecol 155:1–25. https://doi.org/10.1016/0022-0981(92)90024-5

Lucas J (1994) The biology, exploitation, and mariculture of giant clams (*Tridacnidae*). Rev Fish Sci 2:181–223. https://doi.org/10.1080/10641269409388557

Lucas JS, Nash WJ, Crawford CM, Braley RD (1989) Environmental influences on growth and survival during the ocean-nursery rearing of giant clams, *Tridacna gigas* (L.). Aquaculture 80:45–61. https://doi.org/10.1016/0044-8486(89)90272-X

Ma X, Yan H, Fei H, Liu C, Shi G, Huang E, Wang Y, Qu X, Lian E, Dang H (2020) A high-resolution δ18O record of modern *Tridacna* gigas bivalve and its paleoenvironmental implications. Palaeogeog Palaeoclimatol Palaeoecol. 554:109800. https://doi.org/10.1016/j.palaeo.2020.109800

Maxwell RS, Larsson LA (2021) Measuring tree-ring widths using the CooRecorder software application. Dendrochronologia 67:125841. https://doi.org/10.1016/j.dendro.2021.125841

Milano S, Schöne BR, Witbaard R (2017) Changes of shell microstructural characteristics of Cerastoderma edule (Bivalvia) — A novel proxy for water temperature. Palaeogeog Palaeoclimatol Palaeoecol 465:395–406. https://doi.org/10.1016/j.palaeo.2015.09.051

Neo ML, Eckman W, Vicentuan K, Teo SLM, Todd PA (2015) The ecological significance of giant clams in coral reef ecosystems. Biol Conserv 181:111–123. https://doi.org/10.1016/j.biocon.2014.11.004

Pätzold J, Heinrichs JP, Wolschendorf K, Wefer G (1991) Correlation of stable oxygen isotope temperature record with light attenuation profiles in reef-dwelling *Tridacna* shells. Coral Reefs 10:65–69. https://doi.org/10.1007/BF00571825

Payus C, Ann Huey L, Adnan F, Besse Rimba A, Mohan G, Kumar Chapagain S, Roder G, Gasparatos A, Fukushi K (2020) Impact of extreme drought climate on water security in north borneo: case study of Sabah. Water 12:1135. https://doi.org/10.3390/w12041135

Perry CT, Larcombe P (2003) Marginal and non-reef-building coral environments. Coral Reefs 22:427–432. https://doi.org/10.1007/s00338-003-0330-5

R Core Team (2020) R: A language and environment for statistical computing. R Foundation for Statistical Computing, Vienna, Austria. https://www.R-project.org/

Risk M, Sammarco P (1991) Cross-shelf trends in skeletal density of the massive coral Pontes lobata from the Great Barrier Reef. Mar Ecol Prog Ser 69:195–200. https://doi.org/10.3354/meps069195

Roa-Quiaoit HAF (2005) Ecology and culture of giant clams (Tridacnidae) in the Jordanian sector of the Gulf of Aqaba, Red Sea. Dissertation, Universität Bremen

Romanek CS, Grossman EL (1989) Stable Isotope Profiles of *Tridacna* maxima as environmental indicators. Palaios 4:402. https://doi.org/10.2307/3514585

Romanek CS, JonesDS WDF, Krantz DE, Radtke R (1987) Stable isotopic investigation of physiological and environmental changes recorded in shell carbonate from the giant clam *Tridacna* maxima. Mar Biol 94:385–393. https://doi.org/10.1007/BF00428244

Rosewater J (1965) The Family Tridacnidae in the Indo-Pacific. Indo-Pacific Mollusca 1:347–396

Saleh E, Hoque A, Rahman RA (2007) Water circulation in Darvel Bay, Sabah, Malaysia. In: OCEANS 2007–Europe. https://doi.org/10.1109/OCEANSE.2007.4302366

Sano Y, Kobayashi S, Shirai K, Takahata N, Matsumoto K, Watanabe T, Sowa K, Iwai K (2012) Past daily light cycle recorded in the strontium/calcium ratios of giant clam shells. Nat Commun 3:761. https://doi.org/10.1038/ncomms1763

Santodomingo N, Renema W, Johnson KG (2016) Understanding the murky history of the Coral Triangle: Miocene corals and reef habitats in East Kalimantan (Indonesia). Coral Reefs 35:765–781. https://doi.org/10.1007/s00338-016-1427-y

Santodomingo N, Perry C, Waheed Z, Syed Hussein MA, bin, Rosedy A, Johnson KG, (2021) Marine litter pollution on coral reefs of Darvel Bay (East Sabah, Malaysia). Mar Pollut Bull 173:112998. https://doi.org/10.1016/j.marpolbul.2021.112998

Schneider CA, Rasband WS, Eliceiri KW (2012) NIH Image to ImageJ: 25 years of image analysis. Nat Methods 9:671–675. https://doi.org/10.1038/nmeth.2089

Schöne BR (2003) A 'clam-ring' master-chronology constructed from a short-lived bivalve mollusc from the northern Gulf of California, USA. The Holocene 13:39–49. https://doi.org/10.1191/0959683603hl593rp

Schwartzmann C, Durrieu G, Sow M, Ciret P, Lazareth CE, Massabuau JC (2011) In situ giant clam growth rate behavior in relation to temperature: a One-year coupled study of high-frequency noninvasive valvometry and sclerochronology. Limnol Oceanogr 56:1940–1951. https://doi.org/10.4319/lo.2011.56.5.1940

Sully S, Woesik R (2020) Turbid reefs moderate coral bleaching under climate-related temperature stress. Glob Change Biol 26:1367–1373. https://doi.org/10.1111/gcb.14948

Taylor JD, Kennedy WJ, Hall A (1969) The shell structure and mineralogy of the Bivalvia: introduction Nuculacea-Trigonacea. Bull Br Mus Nat Hist Zool 3:1–125

Tedengren M, Blidberg E, Elfwing T (2000) The effects of different light intensities on photosynthesis and filter-feeding of the giant clam, Tridacna squamosa. In: Mollusk research in Asia, Proceedings of the fifth Asian fishery forum 1998. Chiang Mai, Thailand, pp. 165–171

Thompson DJ (1982) Spectrum estimation and harmonic analysis. IEEE Proc 70:1055–1096

Tran D, Perrigault M, Ciret P, Payton L (2020) Bivalve mollusc circadian clock genes can run at tidal frequency. Proc R Soc B 287:20192440. https://doi.org/10.1098/rspb.2019.2440

Veron JEN (2000) Corals of the world, vol 2. Townsville, Australia

Waheed Z, Hoeksema BW (2013) A tale of two winds: species richness patterns of reef corals around the Semporna peninsula. Malaysia Mar Biodiv 43:37–51. https://doi.org/10.1007/s12526-012-0130-7

Warter V, Müller W (2017) Daily growth and tidal rhythms in Miocene and modern giant clams revealed via ultra-high resolution LA-ICPMS analysis — A novel methodological approach towards improved sclerochemistry. Palaeogeog Palaeoclimatol Palaeoecol 465:362–375. https://doi.org/10.1016/j.palaeo.2016.03.019

Warter V, Muller W, Wesselingh FP, Todd JA, Renema W (2015) Late Miocene seasonal to subdecadal climate variability in the Indo-West Pacific (East Kalimantan, Indonesia) preserved in giant clams. Palaios 30:66–82. https://doi.org/10.2110/palo.2013.061

Watanabe T, Suzuki A, Kawahata H, Kan H, Ogawa S (2004) A 60-year isotopic record from a mid-Holocene fossil giant clam (Tridacna gigas) in the Ryukyu Islands: physiological and paleoclimatic implications. Palaeogeog Palaeoclimatol Palaeoecol 212:343–354. https://doi.org/10.1016/S0031-0182(04)00358-X

Watson SA, Neo ML (2021) Conserving threatened species during rapid environmental change: using biological responses to inform management strategies of giant clams. Conserv Physiol 9:coa082. https://doi.org/10.1093/conphys/coab082

Welsh K, Elliot M, Tudhope A, Ayling B, Chappell J (2011) Giant bivalves (Tridacna gigas) as recorders of ENSO variability. Earth Planet Sci Lett 307:266–270. https://doi.org/10.1016/j.epsl.2011.05.032

Yan H, Liu C, An Z et al (2020) Extreme weather events recorded by daily to hourly resolution biogeochemical proxies of marine giant clam shells. Proc Natl Acad Sci USA 117:7038–7043. https://doi.org/10.1073/pnas.1916784117

Yan H, Zhao N, Zhou P, Liu C, Fei H, Li M, Liu F, Yang Y, Yang W, Dodson J (2021) The first detection of the Madden-Julian Oscillation signal in daily to hourly resolution proxy records derived from a natural archive of Giant Clam Shell (Tridacna spp.). Earth Planet Sci Lett 555:116703. https://doi.org/10.1016/j.epsl.2020.116703

Yau AJY, Fan TY (2012) Size-dependent photosynthetic performance in the giant clam Tridacna maxima, a mixotrophic marine bivalve. Mar Biol 159:65–75. https://doi.org/10.1007/s00227-011-1790-8

Yong WLO, Todd PA, Ang ACF et al (2022) Fluted giant clam (Tridacna squamosa) restocking experiment in an urban turbid reef environment. Aquat Conserv Mar Freshw Ecosyst 32:633–644. https://doi.org/10.1002/aqc.3789

Yu X, Salama MHD, Shen F, Verhoef W (2016) Retrieval of the diffuse attenuation coefficient from GOCI images using the 2SeaColor model: a case study in the Yangtze Estuary. Remote Sens Environ 175:109–119. https://doi.org/10.1016/j.rse.2015.12.053

Zhao N, Yan H, Yang Y, Liu C, Ma X, Wang G, Zhou P, Wen H, Qu X, Dodson J (2021) A 237-year long daily growth rate record of a modern giant clam shell from South China Sea and its potential in high-resolution paleoclimate reconstruction. Palaeogeog Palaeoclimatol Palaeoecol 583:110682. https://doi.org/10.1016/j.palaeo.2021.110682

Zweifler A, O'Leary M, Morgan K, Browne NK (2021) Turbid coral reefs: past, present and future—a review. Diversity 13:251. https://doi.org/10.3390/d13060251